Received: 31 March 2021 | Revised: 17 May 2021 | Accepted: 17 May 2021

DOI: 10.1111/ijac.13818

International Journal of Applied Ceramic TECHNOLOGY

SPECIAL ISSUE ARTICLE

Shear properties of C/C-SiC sandwich structures

Bernhard Heidenreich[1] | **Harald Kraft**[1] | **Nathan Bamsey**[2] | **Miguel Such-Taboada**[2]

[1]DLR, Institute of Structures and Design, Stuttgart, Germany

[2]ESTEC, Noordwijk, The Netherlands

Correspondence
Bernhard Heidenreich, DLR, Institute of Structures and Design, D-70569 Stuttgart, Germany.
Email: bernhard.heidenreich@dlr.de

Funding information
ESA, Grant/Award Number: 4000111641/14/NL/PA; DLR

Abstract

Carbon fiber reinforced carbon-silicon carbide (C/C-SiC) sandwich structures have been developed using the Liquid Silicon Infiltration process and the in situ joining method. They offer high mass-specific stiffness, low thermal expansion, and high environmental stability. Potential application areas are highly precise satellite structures, like optical benches. In this study, sandwich samples were manufactured using prepregs based on 2D carbon fibre fabrics and a phenolic resin precursor. Carbon fibre reinforced polymer preforms for folded and grid-cores, as well as for the skin panels were manufactured using autoclave technique. In the second step, the sandwich components were pyrolyzed, leading to C/C preforms. For the build-up of the sandwich samples, two skin panels were joined to a core structure and subsequently, the resulting C/C sandwich preform was siliconized. C/C-SiC sandwich samples were tested under shear load. Shear strength, modulus, and fracture strain were determined and compared to the results obtained by analytical calculation. The shear properties were dependent on the fiber orientation in the core structure as well as on the core type and orientation. The sandwich shear stiffness obtained in the tests was close to the expected theoretical values, calculated on the basis of the material properties and the core geometry.

KEYWORDS

ceramic matrix composites, core-shell structures, joints/joining, sandwich structures

1 | INTRODUCTION

At DLR, the development of carbon fiber reinforced carbon-silicon carbide (C/C-SiC) materials based on the Liquid Silicon Infiltration (LSI) process started in 1988 and was initiated and consistently driven forward by Walter Krenkel and Richard Kochendörfer and their team.[1]

Due to the use of low-cost raw materials and short manufacturing cycles, the LSI method is representing a robust and economic alternative to Chemical Vapour Infiltration and Polymer Infiltration and Pyrolysis processes. LSI-based C/C-SiC and C/SiC are widely used for brake discs and friction pads in automotive and industrial applications, currently representing the most important market for C fiber-based ceramic matrix composites.

From the beginning, the development at DLR was not only focused on the basics of materials and manufacturing processes, but also on the development of structural parts with complex shapes and large geometries. Thereby, lightweight structures like air intake ramps for aeroengines[2] or nose caps for thermal protection systems of re-entry spacecraft,[3,4] as well as high performance brake discs for automobiles and trains, were in the focus.[5] Highly complex structures could be realized by the upscaling of the manufacturing methods for small sample plates to large 3D-shaped shells of up to 740 × 640 × 170 mm^3, as well as by the development of a

tailored in situ joining technology.[6] In addition to parts for high temperature applications, high precision C/C-SiC telescope structures, offering very low coefficient of thermal expansion (CTE) and high geometrical and environmental stability in space, have been developed and were successfully tested in orbit.[7–9]

On the basis of this heritage, novel C/C-SiC sandwich structures have been developed in the past years. Thereby, the sandwich design principle was combined with the cost-effective LSI manufacturing method. The primary aim of this development are lightweight structures for optical benches in space applications. Compared to state-of-the-art materials, like SiC, Zerodur or carbon fibre reinforced polymer (CFRP), the main advantage of C/C-SiC lies in the combination of low density (ρ = 1.9 g/cm³), very low and tailorable CTE, and a quasiductile fracture behavior. Due to the fact that no polymers are existent in C/C-SiC materials and in the joining of the C/C-SiC sandwich structure, no swelling in humidity or outgassing in vacuum is observed, in contrast to sandwich structures based on CFRP. Therefore, highly precise C/C-SiC sandwich parts can be realized, enabling optical set-ups with extreme positioning accuracy. Additionally, mirror blinding caused by outgassing of materials in the extreme vacuum of the space environment is eliminated. Taken as a whole, thin walled, lightweight sandwich structures can be obtained with high mass-specific stiffness and geometrical stability, not influenced by temperature changes or moisture, offering a high potential for the application in optical structures on satellites.

At DLR, C/C-SiC sandwich structures based on different C/C-SiC core types (folded, grid, honeycomb), could be realized by adapting the LSI process parameters for the manufacture of thin-walled core materials and for the in situ joining of filigree cores to the skin panels. Bending samples of different size scales (300 × 50 × 13 mm³, 590 × 100 × 70 mm³) and core types have been manufactured and characterized,[10,11] demonstrating reasonable and predictable mechanical performance, and a high potential for the upscaling of the C/C-SiC sandwich technology to large sized structures, like optical benches. Thereby, no size limits with respect to the LSI process are expected, apart from the geometry of the available furnaces.

Sandwich structures with CFRP skin panels and core structures based on polymer foam or aramid paper honeycomb structures, as well as on grid-cores based on bi- or multidirectional assembled CFRP webs[12,13] are well known. For high temperature applications in sintering furnaces, sandwich structures made of monolithic ceramics[14,15] like alumina and cordierite, are used for charging carriers. They offer high loading capacities at low masses, and finally enable short process cycles for heating up and cooling down, as well as reduced energy consumption.

In this work, the shear properties of C/C-SiC sandwich structures were determined on samples based on different core types, in order to build up a fundamental understanding of the mechanical behaviour of these new core materials, and to provide test data for the evaluation of modelling and simulation methods for the ongoing development of reliable C/C-SiC sandwich structures.

2 | SAMPLE MANUFACTURE

Six different variants of C/C-SiC sandwich samples ($l \times b \times h$ = 72 × 48 × 15 mm³; c = 13 mm) based on different fold and grid-cores were manufactured (Figure 1; Table 1).

In the first step, flat CFRP plates (330 × 300 × t mm³; t = 0.3 and 1 mm) were produced using a resin preimpregnated fabric (prepreg) based on a phenolic resin precursor, named JK 60 at DLR, and a 2D carbon fiber fabric (Toho Tenax HTA40, 3K, twill weave, 245 g/m²) as raw material. For the skin panels (t = 1 mm), three prepreg layers were cut to size and stacked together. The core plates were manufactured with one single prepreg layer (t_c = 0.3 mm). The prepreg lay-up, as well as the single prepreg layer, were densified and cured by autoclave technique ($p_{max.}$ = 0.8 MPa, $T_{max.}$ = 195°C for 1.5 h).

For the manufacture of the CFRP foldcore, one sheet of prepreg was placed in between two release tapes and manually folded step by step, using a foldable master plate.[16]

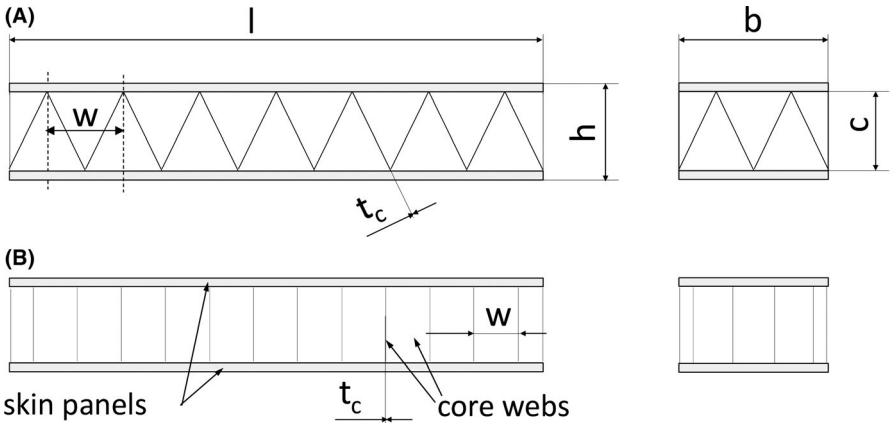

FIGURE 1 Schematic view and nomenclature of sandwich samples with fold (A) and grid-core (B)

TABLE 1 Overview of tested sandwich samples

	F0L	F45L	F0W	F45W	G0	G45
Core type	Fold core				Grid core	
Fibre orientation in web	0°/90°	±45°	0°/90°	±45°	0°/90°	±45°
Core orientation (Figures 2 and 3)	L	L	W	W	—	—
Cell width, w (mm)	16				12	
Core density, ρ_c (kg/m³)	90				74.1	
Number of samples, n	4	4	3	3	3	3

For final forming, the layup was put in a precise, 3D milled mould. After closing the mould, the layup was densified to a defined thickness by applying a uniform pressure of 5.8 kPa, and the prepreg was cured in a furnace ($T_{max.}$ = 220°C, 4.5 h). Two types of foldcores (300 × 300 × 13 mm³) were manufactured, with the fibres oriented in 0°/90° and in ±45°, respectively. Therefore, the prepreg sheets were cut to size with appropriate fiber orientation before folding.

In the second step, the CFRP plates and fold-cores were pyrolyzed at $T_{max.}$ = 1650°C in inert nitrogen atmosphere at ambient pressure. Thereby, the polymer matrix was converted to a carbon matrix, resulting in a porous C/C preform.

Skin panels (300 × 300 × 1 and 72 × 48 × 1 mm³) were cut out of the C/C-plates using a diamond coated saw blade. For the longitudinal and transverse webs of the grid-cores, C/C strips (c = 13 mm; l = 72/48 mm) were cut out with a pulsed fibre laser, offering an average power of 20 W (v = 500 mm/s, 50 cycles; pulse: 26 500 Hz, 200 ns) by Laseric, Stuttgart, now Weinheim. Overall cutting velocity of 10 mm/s was obtained, and a set of 10 strips, needed for the assembly of one sample core, could be cut in less than 5 min. By laser cutting, highly accurate strip width as well as joining slits with a defined width (0.31 mm), spacing (w = 12 mm) and length (l = 0.5 c + 0.1 mm) could be realized. Equidistant slits and close tolerances were mandatory for the subsequent assembly of the strips to the C/C grid-core (Figure 1). In order to investigate the influence of the fibre orientation in the grid-core, the web strips were cut out in parallel to the fibres, and at an angle of 45°, leading to grid-cores with the fibres oriented in 0°/90° (G0) and in ±45° (G45).

For the joining of the C/C core and the skin panels, a joining paste, consisting of JK 60 and a defined content of carbon powder (Timrex® PC 40-OC; Timcal), was used. A certain amount of joining paste was applied homogeneously by dipping the core into a layer of joining paste with defined thickness. Subsequently, the core was placed onto the first skin panel and the joining paste was cured at $T_{max.}$ = 220°C/4 h.

After joining the second skin panel, using the same process, the resulting C/C sandwich structure was siliconized at $T_{max.}$ = 1650°C in vacuum ($p \leq 2$ mbar). Thereby, a homogeneous layer of silicon (Si) granulate was placed on top of the sandwich. At a temperature of about 1425°C, the Si granulate melted, and homogeneously infiltrated the microcrack system of the C/C structure and the joints by capillary forces. In parallel to the infiltration, SiC matrix was built up by a chemical reaction of Si and C at the contact surfaces of the microcracks, finally leading to a dense C/C-SiC material and a permanently jointed C/C-SiC sandwich structure. The multiphase C/C-SiC material is characterized by a typical composition of about 75–80 vol.% of carbon fiber and matrix and 15–20 vol.-% SiC. Residual Si and open porosity is about 1–3 and 1–4 vol.-%, respectively.

The fold-core samples were cut out of the C/C-SiC sandwich panels (300 × 300 × 15 mm³) in W and L-orientation.

3 | SAMPLE TESTING

The sandwich samples were tested by compression, using a compression-loaded double-lap shear test (Figure 3), inspired by ASTM C273 and EN 12090, and an universal testing machine (Zwick/Roell Z100).

Displacement values were determined by using standard travel values, corrected by a calibration curve, which was determined by testing a setup of glued Al plates without sandwich samples.

Shear stress τ and fracture or ultimate shear stress τ_u of the sandwich samples were calculated using Equation (1):

$$\tau = \frac{F}{2} \cdot \frac{1}{b \cdot l}; \tau_u = \frac{F_u}{2} \cdot \frac{1}{b \cdot l}, \quad (1)$$

where F and F_u is the force and ultimate force at fracture, and b and l is the width and length of the sandwich sample, respectively (Figure 1). Shear strain γ und ultimate shear strain γ_u were calculated by using Equation (2), taking into account small displacements f, f_u and the core height c.

$$\tan\gamma = \gamma = \frac{f}{c}; \gamma_u = \frac{f_u}{c}. \quad (2)$$

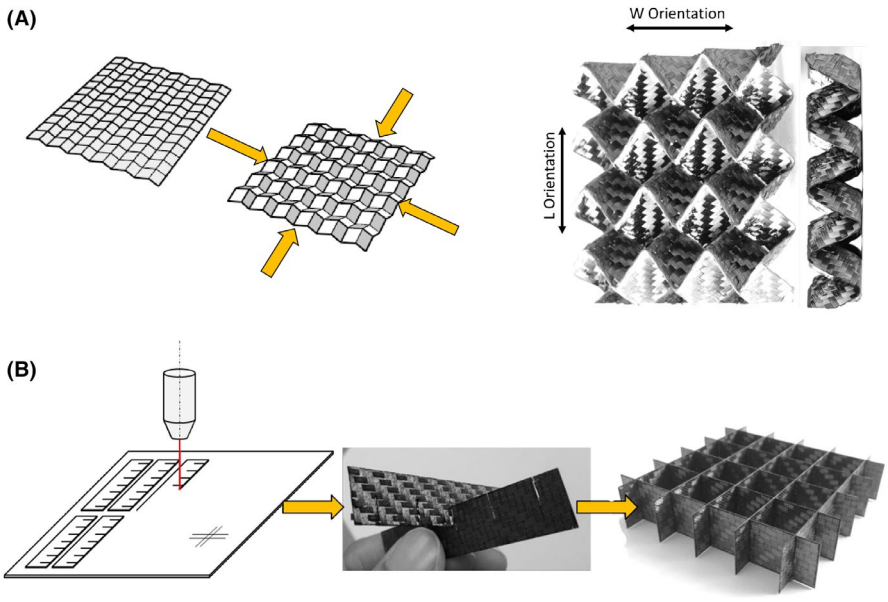

FIGURE 2 Manufacture of a fold-core (A) by folding of a prepreg layer and a grid-core (B) by laser cutting of slit strips out of C/C plates and assembly of the strips to a grid-core

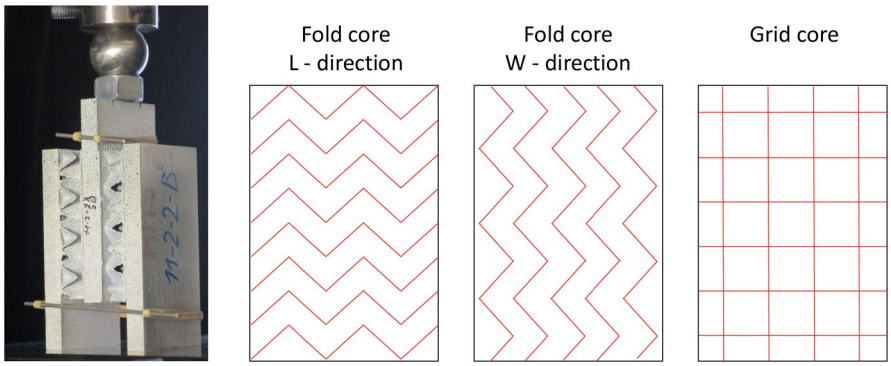

FIGURE 3 Test set-up for in plane shear testing with two sandwich samples glued to three aluminum bars (left), and schematic views of core orientations in the samples

The effective shear modulus $G_{\text{eff.}}$ of the cores was determined from the slope in the linear elastic area of the stress/strain curve. In order to show the effectiveness of the sandwich design, the experimentally achieved results were compared with the theoretically expected values. Therefore, the ultimate shear stress $\tau_{\text{u,web}}$ and the effective shear modulus $G_{\text{eff.,web}}$ of the grid-core webs were calculated using Equations (3 and 4) and were compared to the material properties determined on standard tests of coupons made of similar C/C-SiC materials.

$$\tau_{\text{u,web}} = \frac{F_{\text{u}}}{2} \cdot \frac{1}{n \cdot t_{\text{c}} \cdot l} = \tau_{\text{u}} \frac{b}{n \cdot t_{\text{c}}}, \tag{3}$$

$$G_{\text{eff.,web}} = G_{\text{eff.}} \cdot \frac{b}{n \cdot t_{\text{c}}}. \tag{4}$$

With $t_{\text{c}} = 0.3$ mm is the wall thickness of the core web, and n is the number of core webs, oriented in the load direction. Thereby, only the four grid-core webs, oriented in parallel to the load, were considered.

4 | RESULTS AND DISCUSSION

4.1 | Mechanical properties

In the shear tests, a nonlinear stress/strain behaviour was observed for all samples (Figure 4), and a certain quasiductile behaviour of C/C-SiC sandwich structures under shear load was suggested.

Ultimate shear stress or shear strength of the sandwich samples varied between 0.74 and 1.39 MPa, and was highest for the fold-core based samples, with the core oriented in W-direction and a fiber orientation of ±45° in the core (Figure 5). Generally, a fold-core orientation in W-direction offered 45% and 12% higher shear strength compared to the corresponding samples with the core oriented in L-direction, and fiber orientations of 0°/90° and ±45°, respectively. As expected from laminate theory, a change of the fiber orientation from 0°/90° to ±45° generally lead to an increase of shear strength of 51% and 17% for fold-cores oriented in L- and W-direction, respectively, as well as to an increase of 20% for grid-core based samples. Absolute shear strength

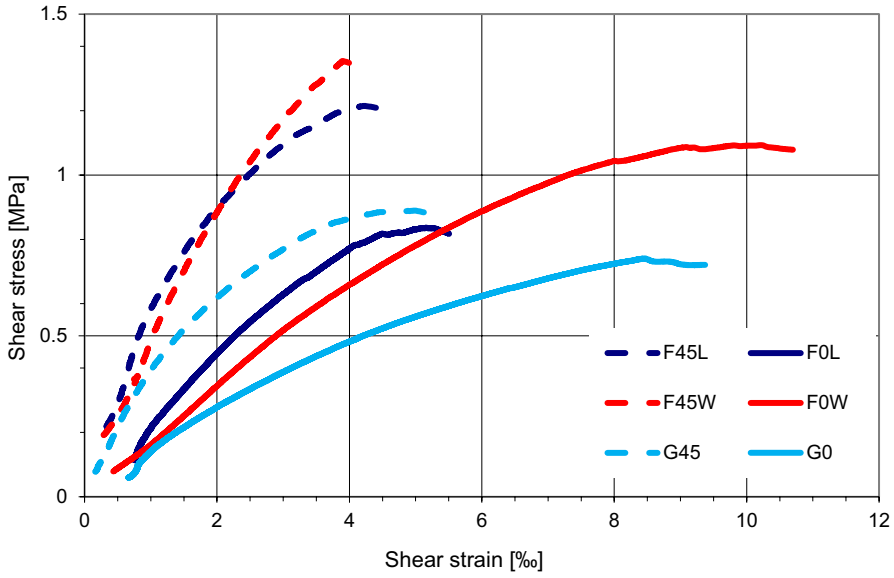

FIGURE 4 Stress/strain behavior of exemplary sandwich samples under shear load

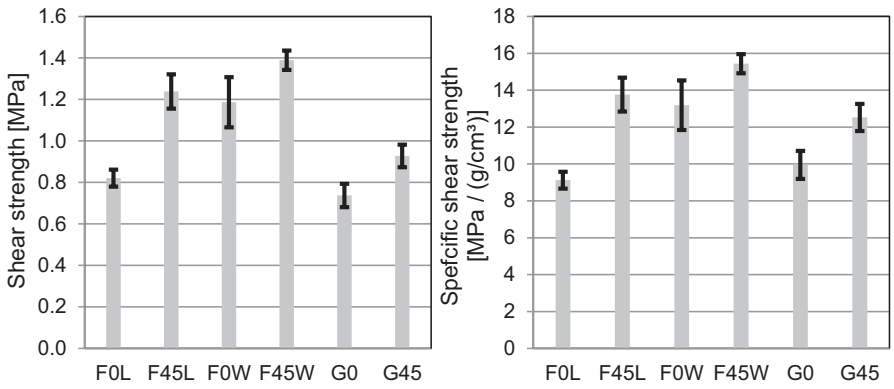

FIGURE 5 Comparison of shear strength and specific shear strength of sandwich samples

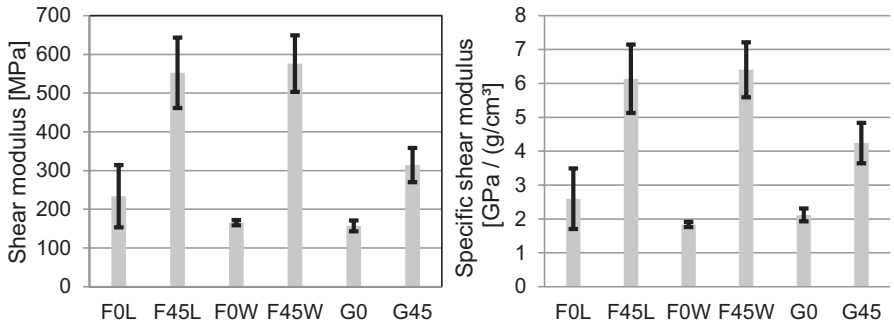

FIGURE 6 Comparison of shear modulus and specific shear modulus of sandwich samples

of grid-core based samples was on a lower level compared to the fold-core–based samples. This was traced back to the lower core density. By comparing the specific shear strength, which is the shear strength divided by the core density, the grid-core based samples showed similar shear strength levels as the fold-core–based sandwich samples in L-orientation.

The effective shear modulus was highest for core materials with ±45° fiber orientation, offering 2.4/3.5 times and 2 times higher values for fold-cores in L/W orientation and grid-cores, respectively, compared to the corresponding samples with 0°/90° fiber orientation (Figure 6), as expected from laminate theory. In contrast, the influence of the fold-core orientation on the shear modulus was quite low, leading to similar values for L and W oriented cores. Whereas the specific shear modulus of the grid-core samples with 0°/90° fibre orientation was similar to the corresponding fold-cores, the grid-core based samples with ±45° fiber orientation showed a 35% lower specific shear modulus compared to the fold-core samples.

Ultimate shear strain increased by a factor of 1.2–2.7 by changing the fiber orientation in the core from ±45° to 0°/90°

(Figure 7), as expected. Highest values were obtained with fold-cores in W-orientation (γ_{FOW} = 10.3‰) and with grid-cores (γ_{GO} = 8.9‰).

Ultimate shear stress in the longitudinal grid-core webs $\tau_{u,web}$ was 29.5 ± 2.3 MPa and 37 ± 2.2 MPa for 0°/90° and ±45° fiber orientation, respectively. These relatively low stress levels in the webs, compared to the shear strength of a typical multilayer C/C–SiC material ($\tau_{u,C/C\text{-}SiC}$ = 80 MPa[17]), was explained by the lower shear strength of a single fabric layer C/C-SiC material, as well as by the stress concentration in the remaining, not slit half of the webs height c. Additionally, an early failure of the thin walled webs (t_c = 0.3 mm) due to buckling, and locally limited or complete failure of the joint between the core structure and the skin panels was estimated to be responsible for the low level of shear stresses obtained in the webs at fracture. Shear modulus of the grid-core webs G_{web} was 7 ± 0.5 GPa for 0°/90° fiber orientation, and increased to 13.4 ± 2.1 GPa when the fibers in the webs were oriented in ±45°, as expected from preliminary tests of typical multilayer C/C–SiC material. Thereby, shear moduli of $G_{C/C\text{-}SiC,0°/90°}$ = 10 GPa and $G_{C/C\text{-}SiC,\pm45°}$ = 16.8 GPa were determined by tension tests of coupons with fibre orientations in ±45°, according to DIN EN ISO 14129.[18]

By comparing these first test results to the values provided for state of the art sandwich core structures[19–23] it becomes apparent that the specific shear modulus of C/C-SiC fold and grid-cores is on a similar level as aluminium or CFRP honeycomb cores, whereas shear strength is comparable to Nomex honeycomb cores based on aramid fiber paper and phenolic polymer matrix (Figure 8).

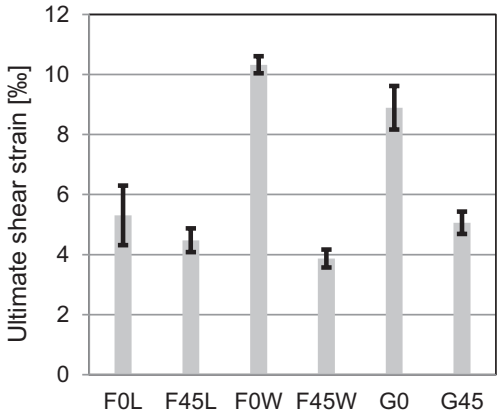

FIGURE 7 Comparison of ultimate shear strain of sandwich samples

4.2 | Failure modes

During the shear test, failure was announced by a distinct emission of cracking noise. However, arising of cracks or crack propagation was not visible with the naked eye, due to a sudden final failure. All fold-core based samples failed by shear cracking of the core (Figure 9). The grid-core based samples also showed shear cracks in parallel to the load. However, additional cracks in the center of the web were observed, which were explained by the buckling of the thin core walls at relatively low loads, as well as by the lower density of the grid-cores compared to the fold-cores. Thereby, the plain and laser cut cell walls of the grid-cores lead to a lower buckling stability, compared to the fold-cores, characterized by uncut fibers and a self-stiffening zig-zag design. For some grid-core samples, also a partial or almost complete debonding between the core structure and the skin panel was observed. This was explained by the low joining area between the grid-core and the skin panel, due to the low wall thickness of the webs, as well as by the butt joint, leading to a perpendicular orientation of the fibers in the web and in the skin panel. In contrast, a parallel fiber orientation in the joining area of the core and the skin panel was achieved with fold-cores, leading to high joining strength. Additionally, due to the angled alignment of the fold-core webs to the skin panels, a meniscus was formed by the joining paste, which significantly increased the width of the joining area, compared to the narrow line joint of the grid-cores.

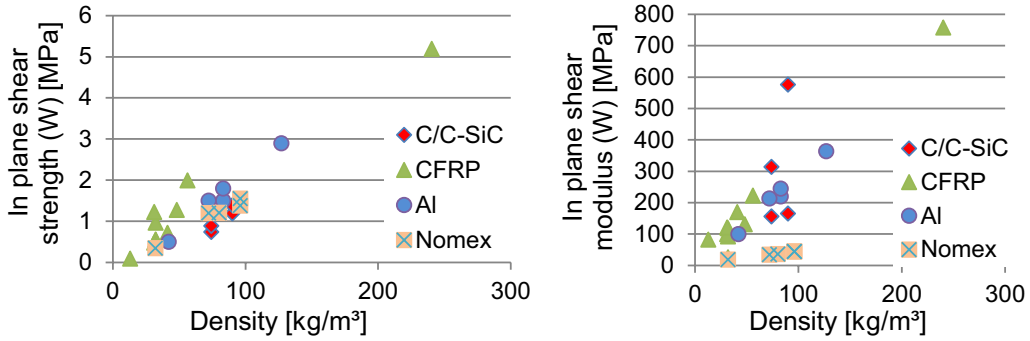

FIGURE 8 Comparison of shear modulus and strength of sandwich samples, based on grid-cores and on fold-cores in W-orientation, with state-of-the-art honeycomb core materials

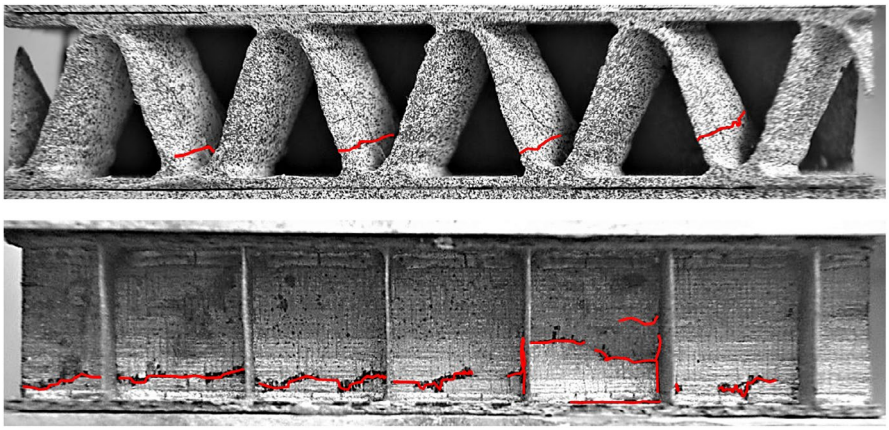

FIGURE 9 Side view of sandwich samples with fold (top) and grid-cores (bottom) after fracture, showing shear cracks in both core types as well as cracks in the center of a grid-core cell, caused by buckling, and partially debonding of skin panel and grid-core (bottom). The cracks are marked in red for better visibility

5 | CONCLUSION

Lightweight C/C-SiC sandwich samples based on fold and grid-cores were manufactured via the LSI process and in situ joining technology. C/C-SiC core structures could be manufactured in near net shape technology by folding a prepreg layer as well as by assembling slit C/C webs, cut out of plane C/C plates via laser beam. Reliable joints between the cores and the skin panels could be achieved by using a dip coating process, ensuring a homogeneous and reproducible application of the joining paste to the face side of the core.

Sandwich samples with fold-cores offered higher specific stiffness and effective shear modulus of up to $G_{\text{eff.}} = 6.4$ GPa/(g/cm³), compared to the sandwich samples based on grid-cores ($G_{\text{eff.}} = 4.2$ GPa/(g/cm³)). The orientation of the fold-cores in L or W direction did not influence the shear modulus of the sandwich samples, leading to an orthotropic behaviour with similar in plane shear stiffness in the main directions, comparable to grid-cores. Whereas shear strength of core materials with ±45° fiber orientation was higher compared to core materials with 0°/90° orientation, a vice versa behaviour for fracture shear strain was observed. After fracture, the grid-core based samples showed buckling effects as well as a failure of the joining, which was traced back to the 21% lower core density, and the reduced joining area compared to fold cores.

Since the stiffness is the most important design criteria for optical benches, whereas the strength and fracture strain are usually not the limiting factors, a fiber orientation of ±45° in the core structure will be mandatory for future C/C-SiC sandwich structures. Fold-cores are preferred, due to their higher specific shear modulus. However, due to design constraints and high manufacturing costs of fold-cores, grid- cores can be advantageous, especially for large structures and core heights. In order to increase the effective shear modulus of grid-cores, core density should be increased by reducing the cell width, or by increasing the wall thickness of the core.

ACKNOWLEDGMENTS

Funding by ESA in the NPI project 318-2013, Contract-No. 4000111641/14/NL/PA is gratefully acknowledged. The authors thank the ESTEC team from Materials Technology Section for the support in mechanical testing and manufacture of test set-up, and the colleagues from DLR, especially Nicole Gottschalk, Felix Vogel, Stefan Frick and Daniel Cepli for sample manufacturing and processing. This work was partially funded by ESA but the main part was funded by DLR.

ORCID

Bernhard Heidenreich https://orcid.org/0000-0002-4330-8844

REFERENCES

1. Krenkel W. Entwicklung eines kostengünstigen Verfahrens zur Herstellung von Bauteilen aus keramischen Verbundwerkstoffen. Doctoral thesis, University of Stuttgart, DLR Forschungsbericht 2000-4; 2000.
2. Kochendörfer R, Krenkel W. CMC intake ramp for hypersonic propulsion systems, in ceramic matrix composites I: design durability and performance. In: Evans AG, Naslain R, editors. High-temperature ceramic-matrix composites. Vol. 57. Abington: Ceramic Transactions; 1995. p. 13–22.
3. Hald H, Weihs H, Benitsch B, Fischer I, Reimer T, Winkelmann P, Gülhan A. Development of a nose cap system for X 38. In *Proceedings of international symposium atmospheric reentry vehicles and systems*, Arcachon, France; 1999.
4. Böhrk H, Elsäßer H, Weihs H. The SHEFEX II thermal protection system, 7th symposium on aerothermodynamics for space vehicles, 9–12 May 2011, Brügge. Belgium: The SHEFEXII Thermal Protection System; 2011.
5. Heidenreich B, Kütemeyer M, Koch D. Development of high performance ceramic brake discs for rail, aircraft and road vehicles. In *Proceedings of EuroBrake*, 13–15 May 2013, Lille, France, FISITA (The International Federation of Automotive Engineering Societies), London; 2014.
6. Krenkel W, Henke T, Mason N. In-situ joined CMC components. Key Eng Mater. 1996;127–131:313–20.
7. Renz R, Heidenreich B, Krenkel W, Schöppach A, Richter F. CMC materials for lightweight and low CTE applications, 4th international conference on high temperature ceramic matrix composites

(HT-CMC 4), München, 1–3 Oktober 2001. In: Krenkel W, Naslain R, Schneider H, editors. High temperature ceramic matrix composites. Weinheim: Wiley-VCH Verlag; 2001, p. 839–45.

8. Schöppach A, Petasch T, Heidenreich B, Renz R, Krenkel W. Use of ceramic matrix composites in high precision laser communication optics. In *Proceedings of the European conference on spacecraft structures, materials and mechanical testing*, held at ESTEC, Nordwijk, The Netherlands, 29 Nov.–1 Dec. 2000, Stavrinidis C, Rolfo A, Breitbach E, editors. European Space Agency, p. 141–145, ESA SP-468, 2001, ESASP.468.141S, March 2001; 2001.
9. Heidenreich M, Scheiffele M, Tausendfreund M, Wieland HU. C/C-SiC telescope structure for the laser communication terminal in TerraSAR-X. In: Krenkel W, Lamon J, editors. High temperature ceramic matrix composites. Berlin: Aviso Verlagsges; 2010, p. 505–12.
10. Heidenreich D, Koch H, Kraft YK. C/C–SiC sandwich structures manufactured via liquid silicon infiltration. J Mater Res. 2017;32:1–11. https://doi.org/10.1557/jmr.2017.208.
11. Heidenreich B, Bamsey N, Shi Y, Such-Taboada M, Koch D. Manufacture and test of C/C–SiC sandwich structures. CEAS Space J. 2020;12:73–84. https://doi.org/10.1007/s12567-019-00263-x.
12. Fan HL, Meng FH, Yang W. Sandwich panels with Kagome lattice cores reinforced by carbon fibers. Compos Struct. 2007;81:533–9. https://doi.org/10.1016/j.compstruct.2006.09.011.
13. Russel BP, Liu T, Fleck NA, Deshpande VS. Quasi-static three-point-bending of carbon fibre sandwich beams with square honeycomb cores. J Appl Mech. 2011;78. https://doi.org/10.1115/1.4003221.
14. Kollenberg W. Customized kiln furniture. Interceram. 2011;60(3–4):208–10.
15. Van Voorhees EJ, Green DJ. Failure behavior of cellular-core ceramic sandwich composites. J Am Ceram Soc. 1991;74:2747–52.
16. Gottschalk N. Entwicklung von C/C-SiC Sandwichbauweisen auf der Basis von Faltstrukturen. Diplomarbeit, University of Stuttgart, Germany; 2014.
17. Hofmann S. Effect of interlaminar defects on the mechanical behaviour of carbon fibre reinforced silicon carbide. Dissertation, Institute of Aircraft Design, University Stuttgart, Germany; 2013.
18. DIN EN ISO 14129, 1998-02. Faserverstärkte Kunststoffe—Zugversuch an 45°-Laminaten zur Bestimmung der Schubspannungs/Schubverformungs-Kurve des Schubmoduls in der Lagenebene (ISO 14129:1997); Deutsche Fassung EN ISO 14129:1997. English title: Fibre-reinforced plastic composites—determination of the in-plane shear stress/shear strain response, including the in-plane shear modulus and strength, by ±45° tension test method (ISO 14129:1997); German version EN ISO 14129:1997. Beuth Verlag, Berlin. 1998.
19. Le C. New developments in honeycomb core materials. Rev 022802. Livermore, CA: Ultracor Inc; 2002. http://www-eng.lbl.gov/~ecanderssen/moisture/Moisture_Adsorption/NewDevelopments.pd. Accessed 31 May 2013.
20. Lengowski M. Entwicklung mechanisch/thermischer Architekturen und innovativer Strukturelemente im Rahmen zweier Satellitenmissionen des Stuttgarter Kleinsatellitenprogramms. Doctoral thesis, University of Stuttgart, Institut für Raumfahrtsysteme (IRS); 2013, p. 120–123.
21. Invent GmbH. CCORE product data, company brochure. Rev. Nr. 300299-TB-01 Issue A. Braunschweig, Germany: Invent GmbH; 2012.
22. Hexcel Corporation. HexWeb HRH-10 Product data sheet, ATU 123 NV17-DS 4000. Stamford, CT: Hexcel Corporation; 2017.
23. Goodfellow. Aluminum honeycomb, online catalogue. March 30, 2021. http://www.goodfellow.com/A/Aluminum-Honeycomb.html. Accessed 30 March 2021.

How to cite this article: Heidenreich B, Kraft H, Bamsey N, Such-Taboada M. Shear properties of C/C-SiC sandwich structures. *Int J Appl Ceram Technol*. 2022;19:54–61. https://doi.org/10.1111/ijac.13818